14 November 1997

ELSEVIER

Chemical Physics Letters 279 (1997) 241–246

CHEMICAL PHYSICS LETTERS

Electron nuclear dynamics of $H^+ + H_2O$ collisions

M. Hedström [1], J.A. Morales, E. Deumens, Y. Öhrn

Quantum Theory Project, Departments of Chemistry and Physics, University of Florida, Gainesville, FL 32611-8435, USA

Received 17 July 1997; in final form 21 August 1997

Abstract

Proton water collisions at 46 eV in the center of mass frame are studied within the electron nuclear dynamics theory (END). The electronic degrees of freedom are described with a coherent state formulation of determinantal wavefunctions. The nuclei are treated as classical particles but full nonadiabatic couplings are retained. The equations of motion are formulated in a generalized phase space and bypass the use of preconstructed potential energy surfaces. Differential cross sections for inelastic and electron transfer reactions as well as energy transfer are compared with experiment. © 1997 Elsevier Science B.V.

1. Introduction

Pioneering time-of-flight studies of low energy proton collisions with a number of small molecular species have been carried out over the past twenty years in the group of Toennies [1–7]. Few theoretical studies have been made of these interesting systems. The proton collisions with hydrogen molecules at 30 eV in the laboratory frame have been studied with the trajectory surface hopping method [8,9] by Toennies' group [5], and by a quantum mechanical study by Baer et al. [10] using diatomics-in-molecule potential energy surfaces. Electron nuclear dynamics (END) calculations [11,12] have also been performed for this system. Excellent agreement was obtained between END and experiment for a whole range of properties including vibrationally resolved differential cross sections.

Larger molecular targets present bigger challenges for theoretical treatments and, thus, fewer quality studies have been made for proton collisions with such systems. END theory has recently been applied to calculate inelastic and electron transfer differential cross sections for proton collisions with methane molecules [13] with results in good agreement with experiment.

In the next section we briefly outline the END theory at its lowest level of approximation. The explicitly dynamical equations that govern the time evolution of the dynamical variables are derived with the principle of least action using a quantum mechanical Lagrangian obtained with an approximate molecular wavefunction. The electrons are described with a Thouless [14] determinant built from complex nonorthogonal spin orbitals expressed in terms of Gaussian basis functions centered on the dynamically moving nuclei. The nuclei are treated as distinguishable particles in terms of Gaussian wave packets in the narrow width limit. In this way the dynamics takes place on a generalized phase space [15] in

[1] Permanent address: Department of Quantum Chemistry, Uppsala University, Box 518, S-751 20 Uppsala, Sweden.

PII S0009-2614(97)01010-5

terms of complex molecular orbital coefficients and average nuclear positions and momenta.

In this Letter we present results of an END study of proton collisions with water at $E_{CM} = 46$ eV. Calculated differential cross sections for inelastic and charge transfer scattering and vibrational energy transfer for the inelastic process are presented together with comparisons with experimental results [6] in Section 3.

2. Theory

The END theory has been developed and compared with other time-dependent methods for molecular processes by Deumens et al. [16], and has been applied to reactive collisions of a number of different systems [17,11,18–21]. The simplest approximation using a complex single Thouless [14] determinant for the electrons and classical nuclei, retaining full electron nuclear coupling, has been implemented in the ENDyne code [22].

The quantum mechanical Lagrangian is

$$L(\psi^*,\psi) = \langle\psi|\mathrm{i}\frac{\partial}{\partial t} - H|\psi\rangle/\langle\psi|\psi\rangle, \tag{1}$$

with H the quantum mechanical Hamiltonian of the system. The choice of the molecular wavefunction $|\psi\rangle$, or rather, family of wavefunctions $|\psi\rangle$, with its particular parametric form in a given basis, constitutes the only approximation of the END theory. Within that approximation full electron nuclear dynamics is considered with instantaneous forces.

The lowest level of approximation within the END theory that makes any sense constitutes the choice of a single product

$$|\psi\rangle = |z,R\rangle|R,P\rangle \equiv |z\rangle|\phi\rangle, \tag{2}$$

of a nuclear wavefunction

$$|R,P\rangle = |\phi\rangle = \prod_k \exp\left[-\frac{1}{2}\left(\frac{X_k - R_k}{a_k}\right)^2 + \mathrm{i}P_k(X_k - R_k)\right] \tag{3}$$

and an electronic part

$$|z,R\rangle = |z\rangle = \det\{\chi_i(x_j)\}, \tag{4}$$

where

$$\chi_i = u_i + \sum_{j=N+1}^{K} u_j z_{ji}, \quad 1 \le i \le N.$$

The spin orbital basis functions $\{u_i(x)\}$ are formed from Gaussians that are centered on the average nuclear positions R_k but carry no average nuclear momentum P_k. It should be noted that the spin orbitals $\{\chi_i\}$ are non-orthogonal and our experience [18,16,12,21,15] is that the complex coefficients $\{z_{ji}\}$, when evolving in time produce a surprisingly flexible description of the participating electrons when also the R'_k and P'_k evolve with the dynamics. The simple product Eq. (2) may be compared to an adiabatic molecular wavefunction, which has the electronic factor depending parametrically on the nuclear coordinate rather than the average nuclear position. In contrast, this simple END wavefunction resembles more a term from the diabatic Born–Huang expansion.

The Euler–Lagrange equations are obtained in matrix form as (see [16,15])

$$\begin{bmatrix} \mathrm{i}C & 0 & \mathrm{i}C_R & 0 \\ 0 & -\mathrm{i}C^* & -\mathrm{i}C_R^* & 0 \\ \mathrm{i}C_R^\dagger & -\mathrm{i}C_R^{\mathrm{T}} & C_{RR} & -I \\ 0 & 0 & I & 0 \end{bmatrix} \begin{bmatrix} \dot{z} \\ \dot{z}^* \\ \dot{R} \\ \dot{P} \end{bmatrix} = \begin{bmatrix} \partial E/\partial z^* \\ \partial E/\partial z \\ \partial E/\partial R \\ \partial E/\partial P \end{bmatrix}, \tag{6}$$

where the limit of narrow nuclear wave packets has been taken, and the definitions of the dynamic metric matrices are

$$(C_{XY})_{ij;kl} = -2\mathrm{Im}\frac{\partial^2 \ln S}{\partial X_{ik}\partial Y_{jl}}\bigg|_{R'=R}, \tag{7}$$

$$(C_{X_{ik}})_{ph} = \frac{\partial^2 \ln S}{\partial z^*_{ph}\partial X_{ik}}\bigg|_{R'=R}, \tag{8}$$

and

$$C_{ph;qg} = \frac{\partial^2 \ln S}{\partial z^*_{ph}\partial z_{qg}}\bigg|_{R=R'}, \tag{9}$$

and where the dot above the symbol denotes time derivative. The overlap between two determinantal wavefunctions is $S = \langle z,\ R'|z,\ R\rangle$, and the total energy $E = \sum_l P_l^2/2M_l + \langle z,R|H_{el}|z,R\rangle / \langle z,R|z,R\rangle$ serves as the generator of infinitesimal time translations.

Transition probabilities are obtained by projecting [12] the evolved state vector, obtained form a given set of initial conditions, against various final states expressed in the same basis. Semiclassical cross sections weighted with these transition probabilities are obtained by integration over initial conditions [23].

3. Results and discussion

All calculations are performed with the ENDyne code [22]. A minimal STO-3G basis is used. Several trajectories are also calculated using a pVDZ basis [24], but no significant differences are observed with the results obtained with the smaller basis. This is in agreement with the experience gained with the ENDyne code in several other applications. The target water molecule is initially at rest in the laboratory frame in its electronic and vibrational ground state. The proton travels towards the water molecule with a momentum commensurate with the chosen collision energy and with an initial impact parameter b. For each trajectory we calculate the angle of deflection of the projectile, $\Theta(b)$ and the probability, $P(b)$, for a certain process, such as charge transfer, to take place. The scattering angle is $\theta = \pm(\Theta - 2n\pi)$ with the sign and integer n are chosen such that $\theta \in [0,\pi]$.

A simple semiclassical cross section is

$$\frac{d\sigma(\theta)}{d\Omega} = \left| \sum_{j=1}^{m} \frac{\sqrt{b_j P(b_j)}}{\sqrt{\sin\theta |d\Theta/db|_{b=b_j}}} e^{iS_j} \right|^2, \qquad (10)$$

where m is the number of trajectories (impact parameters b_j) yielding the same scattering angle and S_j is a semiclassical phase factor. This expression introduces quantum interference and improves on the classical cross section, but diverges at the rainbow angle, θ_r, where $|d\Theta/db|_{b=b_j} = 0$. This divergence is handled using the uniform Airy approximation [25].

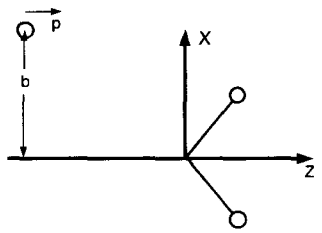

Fig. 1. Reactant initial conditions for the $H^+ + H_2O$ system.

With classical nuclei the initial orientation of the target needs specification. The rotation of the target is labeled by the Euler angles (α, β, γ) about the body-fixed axes. The reference orientation (0, 0, 0) is shown in Fig. 1. Note that the impact parameter is chosen along the positive x-axis. For this application a coarse rotational grid with 36 points is chosen generated from the fourteen target orientations given in Table 1. Averaging over target orientations is then done by numerical quadrature [13] over these grid points.

The overall features of the differential cross section may be determined from considering the deflection function. For scattering angles around and above the rainbow angle an oscillatory behavior of $d\sigma/d\Omega$ is expected, and for even greater angles a decrease is expected since only one branch of Θ contributes. The maxima of the rainbow oscillations are given by the zeros of the Airy function. The first maximum

Table 1
Target orientations in terms of Euler angles. The selected target orientations create 36 grid points for rotational averaging. Rainbow angles and corrected rainbow angles in degrees

Orientation	(α, β, γ)	θ_r	θ_r^{sc}
1	(0, 0, 0)	5.7	4.4
2	(0, 50, 0)	4.9	3.5
3	(0, 130, 0)	4.7	3.3
4	(0, 180, 0)	5.6	4.0
5	(180, 50, 0)	9.5	7.7
6	(180, 130, 0)	9.2	7.8
7	(0, 0, 90)	8.6	7.3
8	(0, 45, 90)	5.5	4.1
9	(0,90, 90)	5.1	4.0
10	(0, 135, 90)	7.8	6.3
11	(0, 180, 90)	8.7	7.3
12	(180, 45, 90)	10.4	8.8
13	(180, 90, 90)	8.2	6.8
14	(180, 135, 90)	7.2	5.6

occurs at the semiclassically corrected rainbow angle θ_r^{sc}.

The general shape of the deflection function may be understood from the nature of the projectile–target interaction. One can discern (Table 1) two major categories of deflection functions, those with $\theta_r < 6°$ and those with $\theta_r > 8°$. For the latter category the incoming proton interacts primarily with the oxygen lone pair and an attractive force dominates for intermediate impact parameters. For the former category the proton interacts primarily with the hydrogens and the less attractive interaction is due primarily to the overlap between the 'empty' orbitals on the proton and those on the water. Orientation 10 represents an intermediate case.

The deflection function behavior for large impact parameters is mainly due to the long-range charge–dipole interaction

$$V(\vec{r}) = \vec{\mu} \cdot \vec{r}/r^3, \qquad (11)$$

with $r = |\vec{r}|$ the distance from the center of the dipole, and $\vec{\mu}$ the target electric dipole moment. From this expression one can see that some target orientations would present a net repulsion to the proton for large impact parameters corresponding to the deflection functions for these orientations going to zero from above, i.e. from positive scattering angles. Other orientations would give rise to a long-range attraction. These somewhat simplistic considerations are confirmed by the detailed END dynamics, where also polarization of the system is taken into account.

3.1. Inelastic collisions

The total differential cross section for the non-transfer inelastic reaction is calculated from Eq. (10) with the uniform Airy approximation with $P(b) = P_{NT}(b)$, being the probability for non-transfer. The calculated values show pronounced rainbow oscillations at 4° in close agreement with the experimental rainbow at 5°. The rotationally averaged result is shown together with the experimental values [6] in Fig. 2. The unnormalized experimental values have been shifted so that the differential cross section at the 5° rainbow angle matches the theoretical value at 4° (the theoretical rainbow angle). The additional theoretical rainbow at 7.5° comes mainly from the

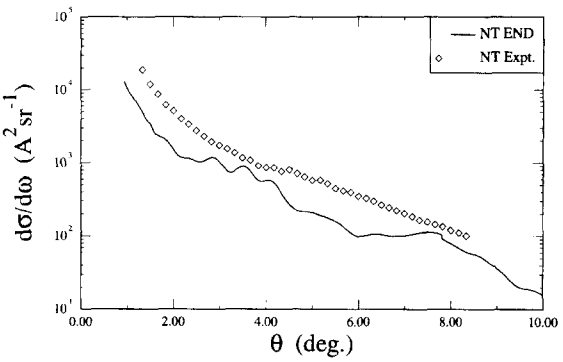

Fig. 2. Inelastic total differential cross section for the $H^+ + H_2O$ collisions at 46 eV.

scattering by the oxygen side of water and is not clearly discernible in the experimental cross section. This may be due to low signal to noise ratio [6]. Even if the theoretical results will be smoothed out by taking into account more target orientations we are confident that the results are reasonably converged. This can be concluded from the behavior of the results with increasing number of target orientations.

The vibrational energy transfer has also been analyzed in the time-of-flight measurements for both inelastic and charge transfer collisions. Theoretical estimates are obtained by projecting the product water molecule state onto the electronic ground state and assuming negligible rotational excitation (experiment estimates rotational excitation to be about 10% of energy loss of the protons). The results presented in Fig. 3 show slightly higher values and are in qualitative agreement with experiment up to 11°.

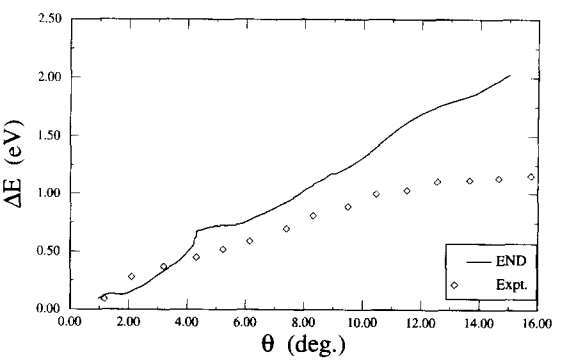

Fig. 3. Vibrational energy transfer ΔE as a function of scattering angle.

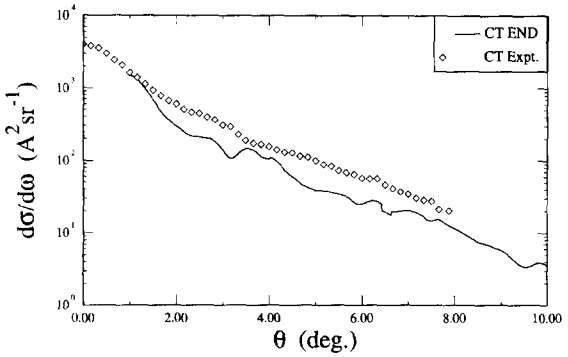

Fig. 4. Charge transfer total differential cross section for the $H^+ + H_2O$ collisions at 46 eV.

3.2. Charge transfer collisions

The differential cross section for charge transfer is calculated in the same way as is done for the inelastic case, but with $P(b) = P_{CT}(b)$, the probability for electron transfer. Again the experimental value at 5° is normalized with the theoretical at 4° and the results are presented in Fig. 4. Due to the difference in detection efficiency for H^+ and H, the experimental data for charge transfer and inelastic scattering, respectively, do not necessarily have the same normalization (see [6]). Therefore the matching of experiment and theory has been done separately for the two cases. The similarities of the charge transfer and the inelastic cross sections in agreement with experiment are manifestations of the similarities between the respective deflection functions. END shows the charge transfer probability to be 1/10 of the inelastic one and the cross section is accordingly an order of magnitude less for the charge transfer case.

4. Conclusions

For this four atom system END gives good agreement with experiment for both inelastic and charge transfer scattering processes. This demonstrates the fact that even at the lowest level of approximation with nonadiabatic couplings taken into account the END wave function behaves satisfactorily. Furthermore, the semiclassical theory introduces the necessary corrections to describe the rainbow oscillations in the differential cross sections.

Acknowledgements

We acknowledge support for the Office of Naval Research. One of us (MH) thanks the Sweden–America Foundation for a scholarship that made his stay at the University of Florida possible. Computations have been performed at the John C. Slater Computing Facility at QTP. Support of this facility by the IBM Corporation through its 1996 SUR program is gratefully acknowledged.

References

[1] K. Rudolph, J.P. Toennies, J. Chem. Phys. 65 (1976) 4483.
[2] W. Eastes, U. Ross, J.P. Toennies, J. Chem. Phys. 70 (1979) 1652.
[3] U. Gierz, M. Noll, J.P. Toennies, J. Chem. Phys. 83 (1985) 2259.
[4] M. Noll, J.P. Toennies, J. Chem. Phys. 85 (1986) 3313.
[5] G. Niedner, M. Noll, J. Toennies, C. Schlier, J. Chem. Phys. 87 (1987) 2686.
[6] B. Friedrich, G. Niedner, M. Noll, J.P. Toennies, J. Chem. Phys. 87 (1987) 5256.
[7] Y.-N. Chiu et al., J. Chem. Phys. 88 (1988) 6814.
[8] A. Bjerre, E.E. Nikitin, Chem. Phys. Lett. 1 (1967) 179.
[9] J.C. Tully, R.K. Preston, J. Chem. Phys. 55 (1971) 562.
[10] M. Baer, G. Niedner-Schatteburg, J.P. Toennies, J. Chem. Phys. 91 (1989) 4169.
[11] Y. Öhrn et al., Time evolution of electrons and nuclei in molecular systems, in: J. Broeckhove, L. Lathouwers (Eds.), Time-Dependent Quantum Molecular Dynamics, Plenum, New York, 1992, pp. 279–292.
[12] J.A. Morales, A.C. Diz, E. Deumens, Y. Öhrn, J. Chem. Phys 103 (1995) 9968.
[13] D. Jacquemin, J.A. Morales, E. Deumens, Y. Öhrn, J. Chem. Phys. (1997), in press.
[14] D.J. Thouless, Nucl. Phys. 21 (1960) 225.
[15] E. Deumens, Y. Öhrn, J. Chem. Soc. Faraday Trans. 93 (1997) 919.
[16] E. Deumens, A. Diz, R. Longo, Y. Öhrn, Rev. Mod. Phys 66 (1994) 917.
[17] E. Deumens, Y. Öhrn, J. Phys. Chem. 92 (1988) 3181.
[18] E. Deumens, A. Diz, H. Taylor, Y. Öhrn, J. Chem. Phys. 96 (1992) 6820.
[19] R. Longo, A. Diz, E. Deumens, Y. Öhrn, Chem. Phys. Lett. 220 (1994) 305.

[20] J.A. Morales, A.C. Diz, E. Deumens, Y. Öhrn, Chem. Phys. Lett. 233 (1995) 392.
[21] Y. Ohrn, J. Oreiro, E. Deumens, Intern. J. Quantum Chem. 58 (1996) 583.
[22] E. Deumens et al., ENDyne software for electron nuclear dynamics, Quantum Theory Prokect, University fo Florida, Gainesville, FL 32611-8435 (1996).
[23] J.N.L. Connor, Semiclassical theory of elastic scattering, in: Semiclassical Methods in molecular scattering and spectroscopy, M.S. Child (Ed.), Nato Advanced Study Institute Series, Reidel, Dordrecht (1979).
[24] T.H. Dunning Jr. J. Chem. Phys. 90 (1989) 1007.
[25] M.V. Berry, Proc. Phys. Soc (London) 89 (1966) 479.